Matter creation cosmology in Brans-Dicke theory: Observational tests and thermodynamic analysis

C. P. Singh[*] and Simran Kaur[†]

Department of Applied Mathematics, Delhi Technological University, Delhi 110042, India

A matter-dominated model with gravitationally induced matter creation is proposed in the framework of Brans-Dicke theory. We obtain the main cosmological functions such as the scale factor of the Universe, the Hubble expansion rate, and the deceleration parameter analytically. We explore the viability of the model to explain the present accelerated expansion of the Universe. In this scenario, the present cosmic acceleration is supposed to be driven only by the negative creation pressure associated with the matter component. The evolution of such a model is tested by statistical analysis of the latest SNe, OHD, and BAO probes. We study and plot the trajectories of the evolution of the Universe with the best estimated values of the model parameters. It is observed that the expanding Universe begins with a big bang followed by a smooth transition from the decelerated phase to the accelerated phase. The ages of the Universe obtained by SNe + OHD and SNe + OHD + BAO in this model are in good agreement with the age predicted by the ΛCDM model. We analyze the model with a statefinder diagnostic and find that the model is different from the ΛCDM model but approaches ΛCDM in the future. The model shows quintessence behavior.

I. INTRODUCTION

A large number of observational data such as type-Ia supernovae [1,2], cosmic background radiation fluctuations [3], and baryon acoustic oscillations [4] have provided strong evidence for an accelerating Universe. The discovery from these observations indicates the existence of a new component with negative pressure, which is generally called dark energy (DE) and is responsible for this acceleration. The simplest candidate of dark energy is the cosmological constant Λ, with equation of state $\omega_\Lambda = -1$ [5]. However, it suffers two well-known problems named the "fine-tuning problem" and the "cosmic coincidence problem" [6]. Such problems have inspired many researchers to propose alternative candidates in the literature: quintessence [7–12], k-essence [13], phantom energy [14–16], quintom [17,18], exotic Chaplygin gas [19], etc., have been proposed in the past 18 years. More recently, some attention has also been paid to a possible interaction between the dark sector components [20–22]. However, the nature of DE is far from being understood.

In the past several years, matter creation in cosmology has drawn the attention of many researchers. After the discovery of the accelerating Universe, matter creation has been reconsidered to explain it and produced some unexpected results. In general relativistic cosmology, the presence of a negative pressure is the key ingredient to accelerating the expansion. Cosmological models dominated by pressureless fluid like a cold dark matter (CDM) component expand in a decelerating way. Matter creation is considered in the context of the thermodynamics of open systems. The first self-consistent theoretical approach to matter creation was proposed by Prigogine and his collaborators [23,24]. It was argued that, at the expense of the gravitational field, matter creation occurs only as an irreversible process constrained by the usual requirements of nonequilibrium thermodynamics. They also showed how the thermodynamics of open systems lead naturally to a reinterpretation of the energy-momentum tensor, adding an additional pressure term. A detailed study of the thermodynamics of matter creation with changing specific entropy has been discussed in Refs. [12,25].

In comparison to the standard equilibrium equations, the irreversible creation process is described by two new ingredients: a balance equation for the particle number density and a negative pressure term in the energy-momentum tensor. Such quantities are related to each other in a very definite way by the second law of thermodynamics. Several interesting features of cosmological models with matter creation have been investigated by many authors [26–34]. This field is very appealing for several important observations carried out in the last ten years. It has been pointed out that models with particle creation can mimic ΛCDM cosmology (see Refs. [29,30,35–39]). Further, Nunes and Pavón [40] have shown that the matter creation models can explain the phantom behavior of the Universe without invoking any phantom fields. Particle

[*]cpsingh@dce.ac.in
[†]skjuneja.maths@gmail.com

creation models in modified theories have recently attracted several authors [41–43].

In recent years, there have also been attempts to model the missing energy of the Universe and to explain its late-time accelerated expansion in purview of the scalar tensor theories where the scalar field is nonminimally coupled to the gravity sector. The pioneering study on scalar-tensor theories was done several decades ago by Brans and Dicke [44], who applied Mach's principle to gravity. It has found a new impetus, as it arises naturally as the low-energy limit of many theories of quantum gravity like superstring theory. Brans-Dicke (BD) theory as a natural extension of Einstein's general theory of relativity passes the experimental tests from the Solar System [45] and explains the accelerated expansion of the Universe [46]. In BD theory, the gravitational constant G is replaced with an inverse-of-time-dependent scalar field, i.e., $G \sim 1/\phi(t)$, which couples to gravity with a coupling parameter ω.

The study of matter creation processes in the context of the cosmological models has recently attracted a lot of interest in cosmology. In this paper, we study the role of irreversible processes, corresponding to the creation of matter out of gravitational energy in BD theory. The aim of this work is to build a cosmological model of late acceleration based on matter creation in the BD theory of gravity. In a flat Friedmann-Robertson-Walker (FRW) geometry, we consider a general creation rate to demonstrate how matter creation explains the accelerating Universe. We obtain the analytical solutions of the Hubble function and the scale factor of the FRW universe. We also constrain the model using the latest compilation of type-Ia supernova data, observational Hubble data, and baryon acoustic oscillation data. We examine the models using independent diagnosis, namely the statefinder parameter from observational constraints. Further, we test the thermodynamic viabilities of the matter creation model.

The paper is organized as follows: In Sec. II, we present the model field equations for matter creation in a flat FRW space-time in BD theory. We obtain the analytical solutions of Hubble parameter and the scale factor in Sec. III. In Sec. IV, we present the solution of the deceleration parameter. In Sec. V, we present a brief introduction of type-Ia supernova data, observational Hubble data, and baryon acoustic oscillation data to test the cosmological model with matter creation in BD theory and derive the constraints on the model parameters. The results obtained by observational data are given in Sec. VI. In Sec. VII, we study the evolution of the Universe with the best fitted values of parameters. We present the thermodynamic analysis of the model in Sec. VIII. Finally, in Sec. IX, we discuss our findings.

II. MODEL AND FIELD EQUATIONS

The action of BD theory in the presence of matter with Lagrangian $\mathcal{L}_m$ in the Jordan frame [47,48] is given by

$$S = \int d^4x \sqrt{(-g)} \left[\frac{1}{16} \left(\phi R - \omega \frac{\nabla_\alpha \phi \nabla^\alpha \phi}{\phi} \right) + \mathcal{L}_m \right], \quad (1)$$

where ϕ is the BD scalar field representing the inverse of Newton's constant, which is allowed to vary with space and time; ω is the generic dimensionless coupling parameter of the theory; and other symbols have their usual meaning.

Let us consider a spatially homogeneous and isotropic flat Friedmann-Robertson-Walker (FRW) line element ($c = 1$),

$$ds^2 = -dt^2 + a^2(t)[dr^2 + r^2(d\theta^2 + \sin^2\theta d\phi^2)], \quad (2)$$

where $a(t)$ is referred to as the scale factor and t is the cosmic time.

The field equations of BD theory derived from the action (1) by varying the action with respect to the metric are given by

$$R_{\mu\nu} - \frac{1}{2} g_{\mu\nu} R = \frac{T_{\mu\nu}}{\phi} + \frac{\omega}{\phi^2} \left[\phi_{;\mu} \phi_{;\nu} - \frac{1}{2} g_{\mu\nu} \phi_{;k} \phi^{;k} \right]$$
$$+ \frac{1}{\phi} [\phi_{;\mu;\nu} - g_{\mu\nu} \Box \phi] \quad (3)$$

and

$$\Box \phi = \frac{T^\mu_\mu}{(2\omega + 3)}, \quad (4)$$

where $T_{\mu\nu}$ is the total energy-momentum tensor $T_{\mu\nu} = T^{(m)}_{\mu\nu} + T^{(c)}_{\mu\nu}$, where $T^{(m)}_{\mu\nu}$ is the energy-momentum tensor for the perfect fluid, i.e.,

$$T^{(m)}_{\mu\nu} = (\rho + p) u_\mu u_\nu + p g_{\mu\nu}, \quad (5)$$

and $T^{(c)}_{\mu\nu}$ is the energy-momentum tensor which corresponds to the matter creation, i.e.,

$$T^{(c)}_{\mu\nu} = p_c (g_{\mu\nu} + u_\mu u_\nu). \quad (6)$$

In the above Eqs. (5) and (6), ρ and p are the energy density and pressure, respectively, and p_c is the creation pressure. In this background, the first nontrivial evolution equation is given by

$$H^2 + H \frac{\dot{\phi}}{\phi} - \frac{\omega}{6} \frac{\dot{\phi}^2}{\phi^2} = \frac{\rho}{3\phi}. \quad (7)$$

The scalar field evolution equation is

$$\ddot{\phi} + 3H\dot{\phi} = \frac{\rho - 3(p + p_c)}{(2\omega + 3)}, \quad (8)$$

where $H = \frac{\dot{a}}{a}$ is the Hubble parameter, and the dot denotes a derivative with respect to cosmic time t. Here, we note that

the case of $\omega = -3/2$ is not allowed. The energy conservation equation $T^{\mu\nu}_{;\nu} = 0$ leads to

$$\dot{\rho} + 3H(\rho + p + p_c) = 0. \tag{9}$$

We work in the Jordan frame. One interesting thing about BD theory in the Jordan frame is that the conservation equation holds for the matter and the scalar field separately. Or, in a slightly different way, the Bianchi identity along with wave equation given by Eq. (8) gives the matter conservation Eq. (9).

In the gravitationally induced matter creation, the usual balance equation $N^{\mu}_{;\mu} = 0$, is modified as [24]

$$N^{\mu}_{;\mu} = n_{;\mu}u^{\mu} + 3Hn = n\Gamma, \tag{10}$$

where $N^{\mu} = nu^{\mu}$ represents the particle flow vector, u^{μ} is the usual particle four-velocity, $n = N/V$ is the particle number density, and Γ is the rate of change of the particle number in a physical volume $V = a^3$ containing N number of particles and has units in time^{-1}. A semicolon denotes a covariant derivative.

It is to be noted that the creation pressure p_c is defined in terms of the creation rate Γ and other physical quantities describing the fluid. In adiabatic particle creation (meaning particles are created but the specific entropy per particle remains constant), the creation pressure is given by [25,27]

$$p_c = -\frac{(\rho + p)}{3H}\Gamma \tag{11}$$

or

$$p_c = -\frac{\rho}{3H}\Gamma \tag{12}$$

for a pressureless ($p = 0$) matter-dominated model. Now, because we consider matter creation, from the second law of thermodynamics, we have the constraint

$$dS = \frac{s}{n}d(nV) \geq 0, \tag{13}$$

where $s = S/V$ is the entropy density.

III. SOLUTION OF FIELD EQUATIONS

Equations (11) and (12) show how the matter creation rate, Γ, modifies the evolution of the scale factor and density of fluid. The evolution of a matter-dominated model can be determined by assuming a suitable form of the creation rate. Although the precise functional form of Γ is still missing, a number of different phenomenological parametrizations have been proposed in the literature. The simplest choices of Γ are $\Gamma \propto H$; however, this model is not consistent with type-Ia supernovae. The other forms of Γ are $\Gamma = H_0$ [38], $\Gamma \propto H^2$ [26], and $\Gamma \propto H^{-1}$ [39]. Steigman

et al. [49] proposed a linear combination in the terms of Hubble parameter as

$$\Gamma = 3\gamma H_0 + 3\beta H, \tag{14}$$

where γ and β are constants contained in the interval [0,1], and H_0 is the present value of H.

At this point, the system of our equations is not closed, and we still have freedom to choose a suitable assumption for the scalar field. In the framework of BD cosmology, the BD scalar field ϕ is usually assumed to have a power-law relation in terms of scale factor [50,51], namely

$$\phi = \phi_0 a(t)^\epsilon, \tag{15}$$

where ϕ_0 and ϵ are constants. Taking the time derivative of Eq. (15), we obtain

$$\frac{\dot{\phi}}{\phi} = \epsilon\frac{\dot{a}}{a} = \epsilon H. \tag{16}$$

Using Eqs. (15) and (16), the first Friedmann equation (7) can be rewritten as

$$\left(1 + \epsilon - \frac{\epsilon^2\omega}{6}\right)H^2 = \frac{\rho}{3\phi_0 a^\epsilon}. \tag{17}$$

From the above Eq. (17), we get

$$2\frac{\dot{H}}{H} = \frac{\dot{\rho}}{\rho} - \epsilon H. \tag{18}$$

Now, from Eq. (9), we obtain

$$\frac{\dot{\rho}}{\rho} = -3\left(1 - \frac{\Gamma}{3H}\right)H. \tag{19}$$

Using Eqs. (19) and (14) in Eq. (18), we get

$$\frac{\dot{h}}{h} + \frac{(\epsilon + 3(1 - \beta))}{2}H_0 h - \frac{3}{2}\gamma H_0 = 0, \tag{20}$$

where $h = \frac{H}{H_0}$ is the dimensionless Hubble parameter. Here H_0 is the present value of the Hubble parameter. Using $\frac{d}{dt} = \frac{\dot{a}}{a}\frac{d}{d\ln a}$, the above equation can be written as

$$h' + \frac{(\epsilon + 3(1 - \beta))}{2}h = \frac{3}{2}\gamma, \tag{21}$$

where the prime denotes a derivative with respect to conformal time $\ln a$.

Performing the integration of Eq. [(21)], we obtain

$$h(a) = \left[\frac{3\gamma}{\epsilon + 3(1 - \beta)} + \left(1 - \frac{3\gamma}{\epsilon + 3(1 - \beta)}\right)\left(\frac{a_0}{a}\right)^{\frac{\epsilon + 3(1 - \beta)}{2}}\right]. \tag{22}$$

From Eq. [(22)], we get the solution of the scale factor $a(t)$ as a function of time:

$$a(t) = a_0\left[1 + \frac{\epsilon + 3(1 - \beta)}{3\gamma}\left(e^{\frac{3\gamma}{2}H_0(t - t_0)} - 1\right)\right]^{\frac{2}{\epsilon + 3(1 - \beta)}}, \tag{23}$$

where a_0 is the present value of the scale factor at cosmic time $t = t_0$, and thereafter we take $a_0 = 1$, and $\epsilon + 3(1 - \beta) \neq 0$, $\gamma \neq 0$. As $(t - t_0) \to 0$, the scale factor $a(t) \to [1 + \frac{\epsilon + 3(1 - \beta)}{2}H_0(t - t_0)]^{\frac{2}{\epsilon + 3(1 - \beta)}}$, which corresponds to early deceleration; and as $(t - t_0) \to \infty$, the scale factor $a(t) \propto e^{\frac{3\gamma}{2}H_0(t - t_0)}$ corresponds to that of the de Sitter universe.

The Hubble parameter in terms of cosmic time t reads

$$H = \frac{H_0 e^{\frac{3\gamma}{2}H_0(t - t_0)}}{[1 + \frac{\epsilon + 3(1 - \beta)}{3\gamma}\left(e^{\frac{3\gamma}{2}H_0(t - t_0)} - 1\right)]}. \tag{24}$$

The Hubble parameter in terms of redshift $1 + z = (a_0/a)$ is given by

$$H(z) = H_0\left[\frac{3\gamma}{\epsilon + 3(1 - \beta)} + \left(1 - \frac{3\gamma}{\epsilon + 3(1 - \beta)}\right)(1 + z)^{\frac{\epsilon + 3(1 - \beta)}{2}}\right]. \tag{25}$$

Using $a(t) = 0$ in Eq. [(23)], we can calculate the cosmic time t_{BB} when the big bang happens:

$$t_{BB} = t_0 + \frac{2}{3\gamma H_0}\ln\left(1 - \frac{3\gamma}{\epsilon + 3(1 - \beta)}\right). \tag{26}$$

The energy density in terms of z is given by

$$\rho = \rho_0(1 + z)^{-\epsilon}\left[\frac{3\gamma}{\epsilon + 3(1 - \beta)} + \left(1 - \frac{3\gamma}{\epsilon + 3(1 - \beta)}\right)(1 + z)^{\frac{\epsilon + 3(1 - \beta)}{2}}\right]^2, \tag{27}$$

where ρ_0 is a constant quantity. The scalar field ϕ has the solution

$$\phi = \phi_0\left[1 + \frac{\epsilon + 3(1 - \beta)}{3\gamma}\left(e^{\frac{3\gamma}{2}H_0(t - t_0)} - 1\right)\right]^{\frac{2\epsilon}{\epsilon + 3(1 - \beta)}}, \tag{28}$$

which shows that the BD scalar field increases exponentially with time.

Let us discuss the matter creation model in the sense of an irreversible process. Adiabatic matter creation means that the total entropy S increases, but the specific entropy (per particle), $\sigma = S/N$, remains constant, i.e., $\dot{\sigma} = 0$, which implies that

$$\frac{\dot{S}}{S} = \frac{\dot{N}}{N}. \tag{29}$$

Now, from $N = na^3$, we have

$$\frac{\dot{N}}{N} = \frac{\dot{n}}{n} + \frac{3\dot{a}}{a}. \tag{30}$$

Inserting Eqs. [(10)] and [(14)] into Eq. [(30)], a straightforward integration yields

$$N(t) = N_0 a^{3\beta} e^{3\gamma H_0(t - t_0)}, \tag{31}$$

where N_0 is the present number of particles. The number of particles is an increasing function of time. Using Eq. [(31)] in Eq. [(29)] and integrating, we get

$$S(t) = S_0 a^{3\beta} e^{3\gamma H_0(t - t_0)}, \tag{32}$$

where S_0 is the present entropy.

The solution for particle number density is given by

$$n = n_0 a^{-3(1 - \beta)} e^{3\gamma H_0(t - t_0)}, \tag{33}$$

which shows that the particle number density first decreases and then increases exponentially with cosmic time t.

The exact solutions coming from Eqs. [(7)] and [(9)] are consistent solutions if they satisfy the wave equation [(8)]. From Eq. [(8)], the conditions of consistency are

$$(2w + 3)(\epsilon - 3(1 - \beta) + 2)\epsilon - (6 + 6\epsilon - \epsilon^2 w)(1 + 3\beta) = 0 \tag{34}$$

and

$$3\epsilon(2w + 3) - (6 + 6\epsilon - \epsilon^2 w) = 0. \tag{35}$$

IV. DECELERATION PARAMETER

The transition from one phase to another can be obtained by defining the deceleration parameter q, which is defined as $q = -a\ddot{a}/\dot{a}^2$. It is straightforward to show from Eq. [(23)] that the deceleration parameter now takes the following form:

$$q(t) = -1 - \left(\frac{3\gamma - 3(1-\beta) - \epsilon}{2} \right) e^{-\frac{3\gamma}{2}H_0(t-t_0)}. \quad (36)$$

Now, eliminating time from Eqs. (23) and (36), and using $a/a_0 = (1+z)^{-1}$, one obtains the deceleration parameter in terms of the redshift:

$$q(z) = \frac{1}{2} \left[\frac{-6\gamma + (1-3\beta+\epsilon)(\epsilon+3(1-\beta)-3\gamma)(1+z)^{\frac{\epsilon+3(1-\beta)}{2}}}{(\epsilon+3(1-\beta)-3\gamma)(1+z)^{\frac{\epsilon+3(1-\beta)}{2}} + 3\gamma} \right]. \quad (37)$$

When $\epsilon + 3(1-\beta) = 3\gamma$, we have $q = -1$ that corresponds to the de Sitter universe. From the above expression, the present-day value of q is

$$q_0 = \frac{1}{2} \left[\frac{-6\gamma + (1-3\beta+\epsilon)(\epsilon+3(1-\beta)-3\gamma)}{\epsilon+3(1-\beta)} \right]. \quad (38)$$

For $\epsilon = 0$, Eq. (37) reduces to the result of Ref. [27] in general relativity. For $\beta = 0$, we find

$$q(z) = \frac{1}{2} \left[\frac{-6\gamma + (1+\epsilon)(3+\epsilon-3\gamma)(1+z)^{\frac{(\epsilon+3)}{2}}}{(3+\epsilon-3\gamma)(1+z)^{\frac{(\epsilon+3)}{2}} + 3\gamma} \right]. \quad (39)$$

Equation (39) shows that the creation of matter is negligible at high redshifts, while due to matter creation at redshifts of the order of a few, a transition from a decelerating to an accelerating phase occurs. For $\gamma = 0$, from Eq. (37) we get

$$q = \frac{1+\epsilon-3\beta}{2}. \quad (40)$$

Equation (40) shows that $\beta = (1+\epsilon)/3$ is a critical value for which $q = 0$. For $\beta < (1+\epsilon)/3$, the possible values of $q(z)$ are always constant and positive, while for $\beta > (1+\epsilon)/3$, they remain constant and negative in the course of expansion. There is no transition from the deceleration to the acceleration phase.

The transition redshift z_{tr} can be obtained by taking $q = 0$ in Eq. (37), which implies that

$$z_{tr} = \left[\frac{6\gamma}{(1+\epsilon-3\beta)(\epsilon+3(1-\beta)-3\gamma)} \right]^{\frac{2}{(\epsilon+3(1-\beta))}} - 1. \quad (41)$$

Note that the case $\gamma = 0$ gives $z_{tr} = -1$, which shows that the transition would be in the infinite future. This gives a contradiction with SNe data. Equation (41) equivalently can be written as

$$\gamma = \frac{1}{3} \frac{(1+\epsilon-3\beta)(\epsilon+3(1-\beta))(1+z_t)^{\frac{(\epsilon+3(1-\beta))}{2}}}{2 + (1+\epsilon-3\beta)(1+z_t)^{\frac{(\epsilon+3(1-\beta))}{2}}}. \quad (42)$$

For $\beta = 0$, the above expression gives

$$\gamma = \frac{1}{3} \frac{(1+\epsilon)(\epsilon+3)(1+z_t)^{\frac{(\epsilon+3)}{2}}}{2 + (1+\epsilon)(1+z_t)^{\frac{(\epsilon+3)}{2}}}. \quad (43)$$

V. OBSERVATIONAL DATASETS

In this section, we use the Hubble parameter (25) to perform three different statistical analyses involving the latest observational data—namely, type-Ia supernovae (SNe), observational Hubble parameter data, (OHD) and baryon acoustic oscillation (BAO)—to obtain the best fit of the model parameters—namely, ϵ, β, and γ. The goodness of fit of the model is obtained by the χ^2 minimization and likelihoods by using a Markov chain Monte Carlo (MCMC) method [52]. In this study, we have taken the value of the Hubble constant to be $H_0 = 67.8$ km sec^{-1} Mpc^{-1} [53].

A. Supernovae type Ia

We use the joint light-curve analysis (cJLA) dataset of 31 check points (30 bins) covering the redshift range $z = [0.01, 1.3]$ [54]. In a flat universe, the luminosity distance $d_L(z)$ is defined as

$$d_L(z, H_0, \theta) = c(1+z) \int_0^z \frac{dz'}{H(z', \theta)}, \quad (44)$$

where $H(z)$ is defined in Eq. (25), θ denotes the model parameters—namely ϵ, β, and γ—and c is the speed of light given in units of km/sec.

The theoretical distance modulus is defined as

$$r = \mu_b - M - 5\log_{10} d_L, \quad (45)$$

where μ_b is the observational distance modulus and M is a free normalization parameter. We construct the statistical χ^2 function as

$$\chi^2_{\text{SNe}} = r^t C_b^{-1} r, \quad (46)$$

where C_b is the covariance matrix of μ_b; see Table F.2 of Ref. [54]. We numerically minimize χ^2 to compute the *best estimates* for free parameters $(\epsilon, \beta, \gamma)$ of the model.

B. Observational Hubble data

The observational Hubble data are based on differential ages of the galaxies [55]. We use the OHD dataset of 43 measurement points collected in Ref. [56] in the redshift range $0 < z < 2.5$. The best-fit values of the model parameters are determined by minimizing

TABLE I. The best-fit results of model parameters obtained from the analysis with different combinations of the datasets.

Dataset	ϵ	β	γ	M	χ^2_{min}
SNe	$1.898^{+0.633}_{-0.535}$	$0.667^{+0.210}_{-0.240}$	$0.645^{+0.218}_{-0.240}$	$24.941^{+0.020}_{-0.022}$	18.427
SNe + OHD	$2.142^{+0.593}_{-0.698}$	$0.512^{+0.205}_{-0.224}$	$0.840^{+0.066}_{-0.079}$	$24.945^{+0.018}_{-0.020}$	28.223
SNe + BAO	$1.915^{+0.665}_{-0.651}$	$0.448^{+0.225}_{-0.199}$	$0.813^{+0.072}_{-0.059}$	$24.932^{+0.021}_{-0.020}$	17.497
SNe + OHD + BAO	$2.141^{+0.596}_{-0.672}$	$0.597^{+0.200}_{-0.215}$	$0.731^{+0.021}_{-0.020}$	$24.951^{+0.017}_{-0.018}$	30.671

$$\chi^2_{\text{OHD}} = \sum_{i=1}^{m} \frac{[H(z_i) - H_{\text{obs}}(z_i,\theta)]^2}{\sigma_i^2}, \qquad (47)$$

where $H(z_i)$ and $H_{\text{obs}}(z_i)$ are the theoretical and observed values, respectively, and σ_i^2 is the standard deviation of each $H_{\text{obs}}(z_i)$.

C. Baryon acoustic oscillations

We use BAO measurements from SDSS(R) [57], the 6dF galaxy survey [58], BOSS CMASS [59], and three parallel measurements from the WiggleZ survey [60].

The angular diameter $d_A(z,\theta)$ is given by

$$d_A(z_*,\theta) = c \int_0^{z_*} \frac{dz'}{H(z',\theta)}, \qquad (48)$$

where z_* denotes the photons decoupling redshift and according to the Planck 2015 results [53], its value is $z_* \approx 1090$. Further, the dilation scale $D_v(z,\theta)$ is given by $D_v(z,\theta) = \left(\frac{d_A^2(z,\theta)cz}{H(z,\theta)}\right)^{\frac{1}{3}}$.

The corresponding χ^2 function is given by [61]

$$\chi^2_{\text{BAO}} = A^T C^{-1} A, \qquad (49)$$

where A is a matrix given by

$$A = \begin{bmatrix} \frac{d_A(z_*,\theta)}{D_v(0.106,\theta)} - 30.84 \\ \frac{d_A(z_*,\theta)}{D_v(0.35,\theta)} - 10.33 \\ \frac{d_A(z_*,\theta)}{D_v(0.57,\theta)} - 6.72 \\ \frac{d_A(z_*,\theta)}{D_v(0.44,\theta)} - 8.41 \\ \frac{d_A(z_*,\theta)}{D_v(0.6,\theta)} - 6.66 \\ \frac{d_A(z_*,\theta)}{D_v(0.73,\theta)} - 5.43 \end{bmatrix}$$

and C^{-1} is the inverse of the covariance matrix [61]. Here, we have adopted the correlation coefficients given in Ref. [62].

VI. RESULTS

In our analysis, we perform a global fitting to determine the model parameters using the MCMC method. We have adopted a Python implementation of the ensemble sampler for MCMC, EMCEE, introduced by Foreman-Mackey et al. [52]. Table I summarizes the best-fit values of model parameters obtained by statistical analysis carried out using different sets of observational data. The results of SNe and SNe + BAO are little different from those of SNe + OHD and SNe + OHD + BAO.

In statistical analysis, we find the best-fit values of model parameters at $1\sigma(68.3\%)$ and $2\sigma(95.4\%)$ confidence levels, satisfying the constraints $0 < \epsilon < 3, 0 < \beta < 1, 0 < \gamma < 1$, and $1 < (\beta + \gamma) < 2$. We can test the reliability by comparing the result with a spatially flat ΛCDM model. We observe that the model provides a very good fit to these data. Figures 1–4 show confidence contours on parameters and the marginalized likelihood function of the model obtained from the combined analysis with different datasets. The best-fit values of model parameters are given in Table I.
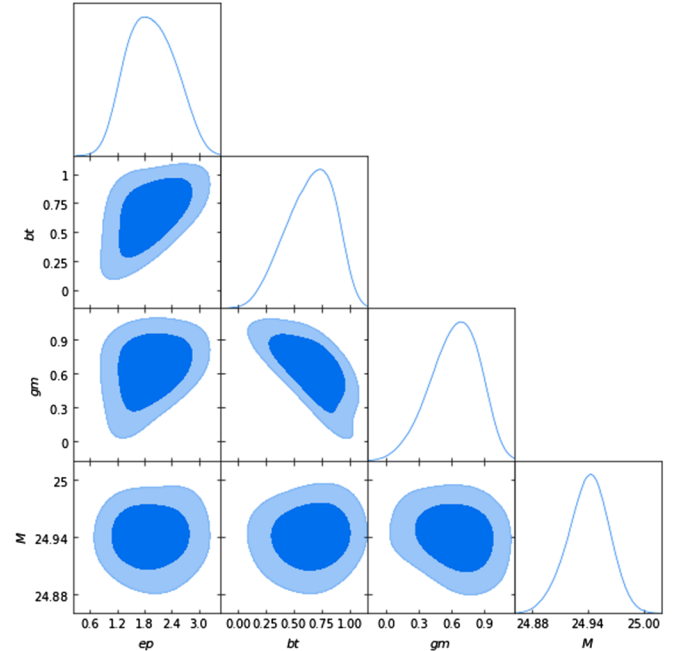

FIG. 1. The contour map of a matter creation model using data from SNe with marginalized probability for the parameters. The associated 1σ and 2σ confidence contours are shown. The labels ep, bt, and gm denote ϵ, β, and γ parameters, respectively.
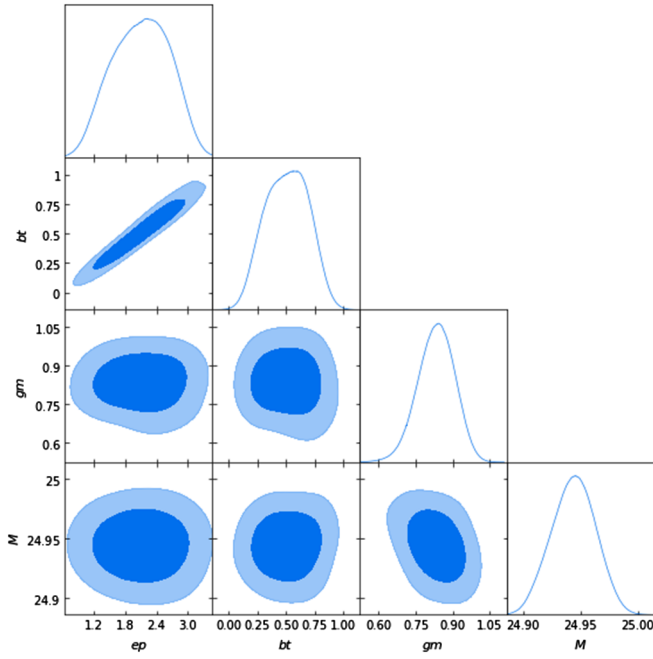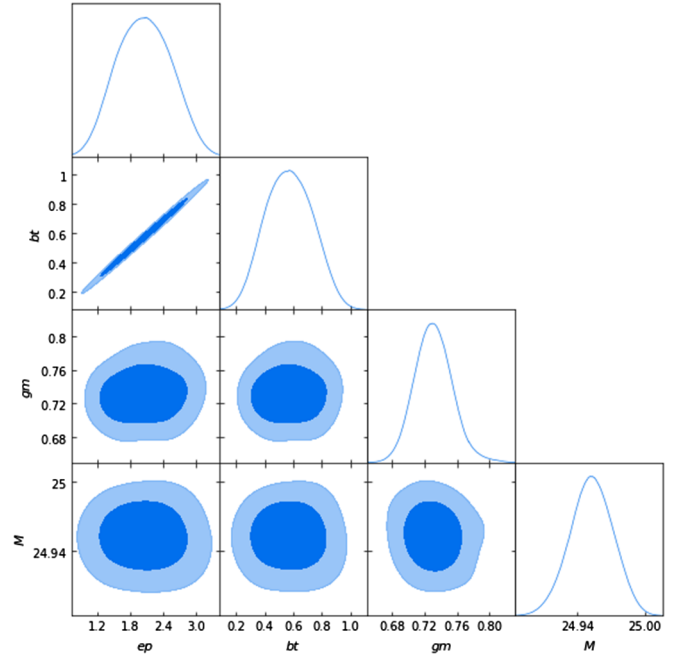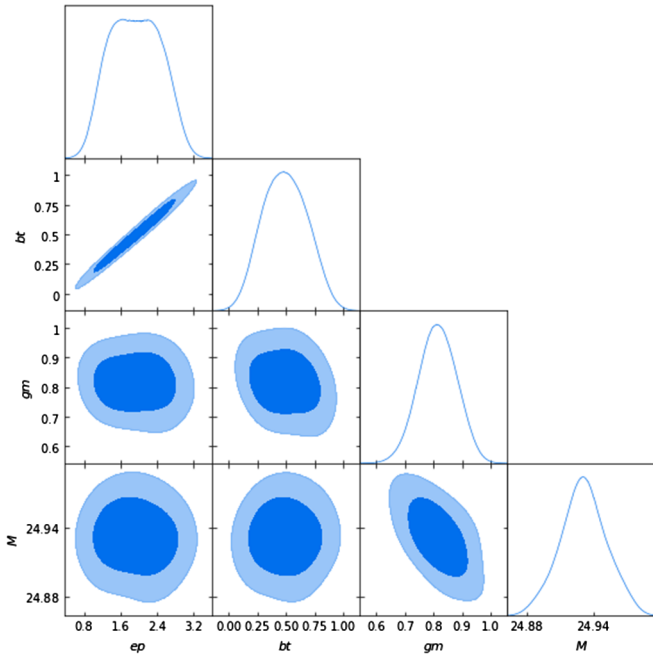
FIG. 2. The contour map of a matter creation model based on joint analysis of SNe + OHD, showing contours of $1\sigma(68.3\%)$ and $2\sigma(95.4\%)$ regions with marginalized probability for the parameters. The labels ep, bt, and gm denote ϵ, β, and γ parameters, respectively.

FIG. 4. The contour map of a matter creation model based on joint analysis of SNe + OHD + BAO, showing contours of $1\sigma(68.3\%)$ and $2\sigma(95.4\%)$ regions with marginalized probability for the parameters. The labels ep, bt, and gm denote ϵ, β, and γ parameters, respectively.

VII. EVOLUTION OF THE MODEL

In this section, we discuss the evolution of the different cosmological quantities using the best-fit values of model parameters obtained from different observational datasets. Figure 5 shows the evolution of the scale factor for different values of model parameters using observational data. It shows that the model starts expansion with an accelerated rate at early time. The dots denote the transition point where the Universe transits from deceleration to the
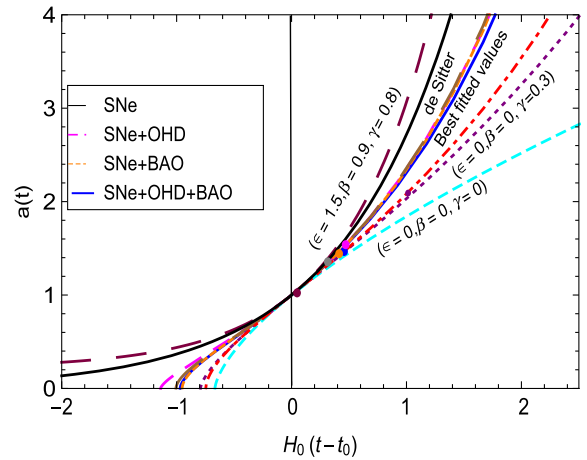

FIG. 3. The contour map of a matter creation model based on joint analysis of SNe + BAO, showing contours of $1\sigma(68.3\%)$ and $2\sigma(95.4\%)$ regions with marginalized probability for the parameters. The labels ep, bt, and gm denote ϵ, β, and γ parameters, respectively.

FIG. 5. The scale function as a function of time for different values of model parameters ϵ, β, and γ. The dots show the transition point.

TABLE II. The transition scale factor, redshift, and present values of the deceleration parameter and the equation of state parameter using best-fit results of model parameters.

Data	a_{tr}	z_{tr}	q_0	$w_{eff}(z)$
SNe	0.3548	1.8180	−0.779	−0.679
SNe + OHD	0.5551	0.8013	−0.457	−0.638
SNe + BAO	0.4986	1.005	−0.434	−0.662
SNe + OHD + BAO	0.5398	0.8522	−0.422	−0.614

acceleration phase. We have also plotted the trajectories for other different values of parameters. The bottom curve gives the trajectory without matter creation ($\beta = 0$, $\gamma = 0$) in general relativity ($\epsilon = 0$), which clearly shows the expansion in the decelerated rate.

To compute the value of the scale factor where transition happens, we have from Eq. (25)

$$\frac{d\dot{a}}{da} = \frac{H_0}{(\epsilon + 3(1-\beta))}$$
$$\times \left[3\gamma + \frac{(\epsilon + 3(1-\beta-\gamma))(2-\epsilon-3(1-\beta))}{2} a^{-\frac{\epsilon+3(1-\beta)}{2}} \right].$$
(50)

Equating Eq. (50) to zero, we get

$$a_{tr} = \left[\frac{(\epsilon + 3(1-\beta-\gamma))(\epsilon + 3(1-\beta) - 2)}{6\gamma} \right]^{\frac{2}{\epsilon+3(1-\beta)}}, \quad (51)$$

where the subscript "tr" denotes the transition. The values of a_{tr} are listed in Table II for different values of model parameters. In the expression (23), If we assume $\epsilon + 3(1-\beta) = 3\gamma$, we obtain the de Sitter universe $a(t) = e^{H_0(t-t_0)}$ as shown in Fig. 5 by the solid black line. In this case, the model predicts an eternal accelerated expansion. For $0 < \epsilon + 3(1-\beta) < 3\gamma$, the model expands forever (see the brown curve), and for $\epsilon + 3(1-\beta) > 3\gamma$, we find that the model begins with a big bang followed by an eternal expansion.

Using the best-fitting data of the parameters listed in Table I in Eq. (37), the variation of q with z is shown in Fig. 6. It is observed that the evolutions corresponding to the best estimates from all observational data are identical. The deceleration parameter starts from negative redshift, $z = -1$, and takes the transition from negative to positive. The model transits from the decelerated to the accelerated epoch at around $z_{tr} \sim 0.8$ with SNe + OHD and SNe + OHD + BAO, whereas SNe and SNe + BAO predict the transition at around $z \sim 1.818$ and $z \sim 1.005$, respectively, which is significantly higher and hints at a strong deviation from the other two. The transition redshift z_{tr}, at which q enters the negative region, and the present-day value of q_0 are given in Table II. The present-day
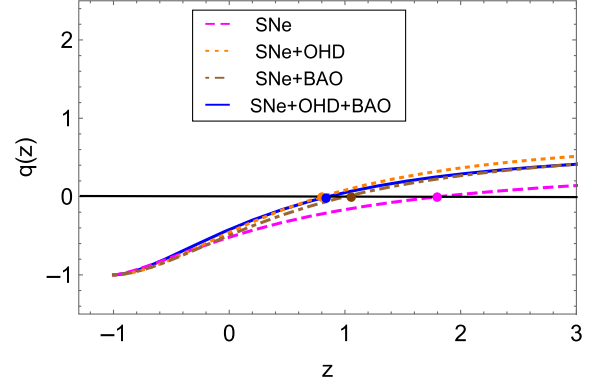

FIG. 6. The evolution of the deceleration parameter $q(z)$ vs redshift z for the best estimated values of parameters. The dot denotes the value of z_t at which $q(z) = 0$, as mentioned in Table II.

negative value $-1 < q_0 < 0$ with each observational data shows that the model behaves like quintessence.

The effective equation of state parameter, ω_{eff}, can be obtained using the standard relation [63]

$$\omega_{eff} = -1 - \frac{1}{3} \frac{2a}{h} \frac{dh}{da}, \quad (52)$$

where $h = H/H_0$ is the weighted Hubble parameter. Using Eq. (22) in Eq. (48), we get

$$\omega_{eff} = -1 + \frac{1}{3} \frac{(\epsilon + 3(1-\beta-\gamma))(1+z)^{\frac{(\epsilon+3(1-\beta))}{2}}}{h}. \quad (53)$$

As $z \to -1$ ($a \to \infty$), we get $\omega_{eff} \to -1$, which can also be observed from Fig. 7. This means that the model corresponds to ΛCDM in future time. The equation of state does not cross the phantom divide line $\omega \leq -1$, which shows that the matter creation model is free from big-rip singularity.
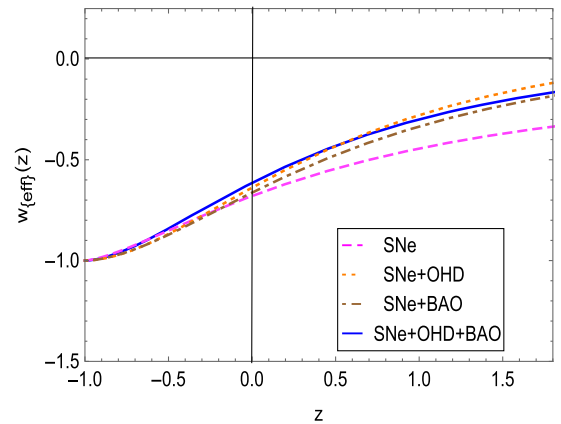

FIG. 7. Plot of effective equation of state parameter ω_{eff} with respect to the redshift z for best-fitted parameters.
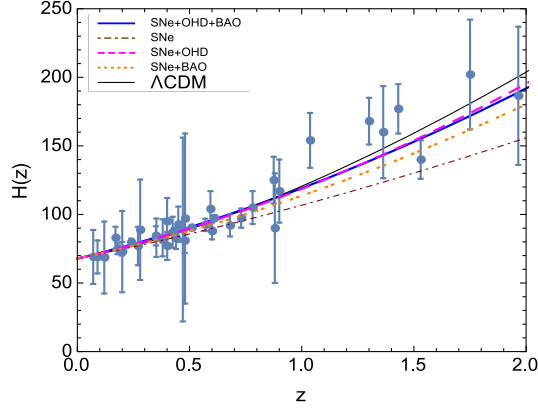
FIG. 8. The Hubble function in terms of the redshift for the ΛCDM model and the fitted model with error bar plots from Hubble data.

The present value ($h = 1$) of ω_{eff} is found to be

$$\omega_{\text{eff}}(z = 0) = -1 + \frac{\epsilon + 3(1 - \beta - \gamma)}{3}. \tag{54}$$

The present values of ω_{eff} are listed in Table II using different observational data. These values are comparatively higher than that predicted by the joint analysis of WMAP + BAO + H_0 + SNe data, which is around -0.93 [64].

We compare our model with the ΛCDM model with the error bar plots of Hubble dataset in the range $z\epsilon(0, 2)$ as shown in Fig. 8. Although at the low redshifts the curves coincide, their evolution with increasing z differs appreciably in the cases of SNe and SNe + BAO. However, it is possible to get a good fit using joint statistical analysis of SNe + OHD and SNe + OHD + BAO.

We calculate the age of the Universe. The age of our Universe at redshift z is given by $t(z) = T(z)/H_0$, where

$$T(z) = \int_z^\infty \frac{dz'}{(1 + z')(H(z)/H_0)} \tag{55}$$

is the dimensionless age parameter. For the ΛCDM model, in which the density parameter, $\Omega_{m0} \approx 0.27$, the age parameter is [65]

$$T(z) = \int_z^\infty \frac{dz'}{(1 + z')[\Omega_{m0}(1 + z)^3 + (1 - \Omega_{m0})]^{1/2}}. \tag{56}$$

It is to be noted that the present age of the Universe for a flat CDM model dominated by matter [$\Omega_{m0} = 1$, $t_0 = 2/(3H_0)$] gives $t_0 \approx 8$–10 Gyr, which does not satisfy the stellar age bound, $t_0 > 11$–12 Gyr; namely, the age of the Universe should be longer than any objects living in the Universe. Therefore, this model suffers the age problem. However, for the ΛCDM model, it easily satisfies the constraint $t_0 > 11$–12 Gyr. A plot of the age of the Universe with redshift for the best estimates of model parameters is shown in Fig. 9. The age of the Universe
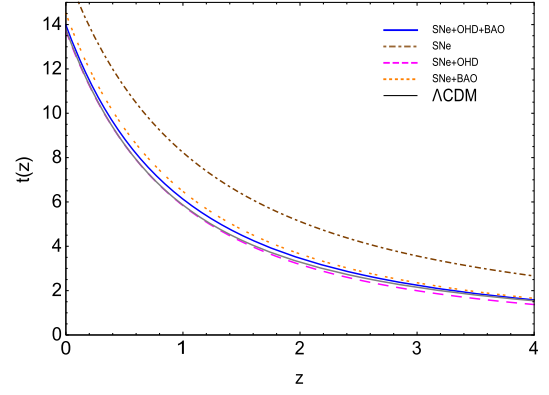

FIG. 9. The age of the Universe for best-fitted values and the ΛCDM model in units of Gyr with redshift.

corresponding to SNe + OHD and SNe + OHD + BAO is found to be 13.9 Gyr. So, the age predicted by the present model is agreeing with the age deduced from the ΛCDM model, which is around 13.799 ± 0.021 Gyr.

To compare with the ΛCDM model, we have used the statefinder parameter diagnostic introduced by Sahni *et al.* [66]. The statefinder parameters $\{r, s\}$ are defined as

$$r = \frac{\dddot{a}}{aH^3} \quad \text{and} \quad s = \frac{r - 1}{3(q - 1/2)}. \tag{57}$$

For the ΛCDM and standard cold dark matter (SCDM), these parameters constitute fixed points $\{r, s\} = \{1, 0\}$ and $\{r, s\} = \{1, 1\}$, respectively, in $s - r$ plane. For our model, the statefinder parameters are given by

$$\begin{aligned}
r &= \frac{(2 - (\epsilon + 3(1 - \beta)))(2 - 2(\epsilon + 3(1 - \beta)))}{4} \\
&+ \frac{9\gamma}{4}(2 - (\epsilon + 3(1 - \beta)))e^{-\frac{3\gamma H_0}{2}(t - t_0)} \\
&\times \left[1 + \frac{\epsilon + 3(1 - \beta)}{3\gamma}\left(e^{\frac{3\gamma H_0}{2}(t - t_0)} - 1\right)\right] \\
&+ \frac{9\gamma^2}{4}e^{-3\gamma H_0(t - t_0)}\left[1 + \frac{\epsilon + 3(1 - \beta)}{3\gamma}\left(e^{\frac{3\gamma H_0}{2}(t - t_0)} - 1\right)\right]^2,
\end{aligned} \tag{58}$$

$$s = \frac{(r - 1)}{3\left[-\frac{3}{2} + \left(\frac{3\gamma - 3(1 - \beta) - \epsilon}{2}\right)e^{-\frac{3\gamma}{2}H_0(t - t_0)}\right]}. \tag{59}$$

We observe that as $(t - t_0) \to \infty$, $\{r, s\} \to \{\frac{(3\beta - \epsilon - 1)(3\beta - \epsilon - 2)}{2}, \frac{2(1 - r)}{9}\}$, which deviates from the ΛCDM model. However, it corresponds to the ΛCDM model for $\epsilon = 0$ and $\beta = 0$. The $\{r, s\}$ plane trajectory of the model for the best estimated values of parameters by SNe + OHD + BAO is shown in Fig. 10. The plot lies in the region $r < 1$, $s > 0$, which is the general behavior of any quintessence model. The $\{r, q\}$ trajectory of the model is
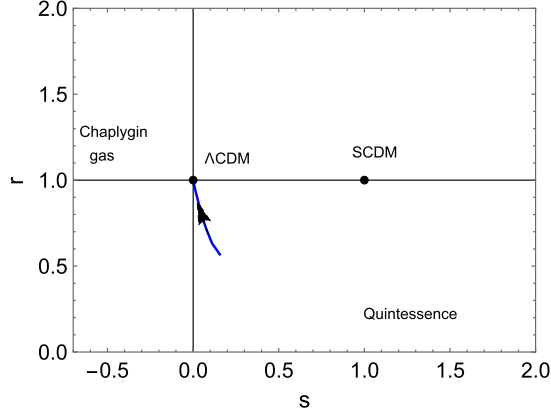
FIG. 10. The trajectory of $\{r, s\}$ in the $s-r$ plane corresponds to the best-fitted parameters obtained from joint analysis of SNe + OHD + BAO. The arrow shows the direction of the evolution of the trajectory.
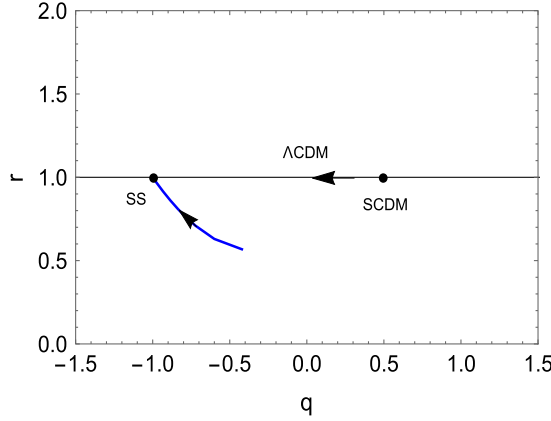

FIG. 11. The trajectory of $\{r, q\}$ in the $q-r$ plane for the best-fitted parameters obtained from joint analysis of SNe + OHD + BAO. The arrow shows the direction of the evolution of the trajectory.

shown in Fig. 11. The SCDM model and steady state (SS) model correspond to the fixed points $\{r, q\} = \{1, 0.5\}$ and $\{r, q\} = \{1, -1\}$, respectively. The horizontal line at $r = 1$ corresponds to the time evolution of the ΛCDM model. Our model approaches the standard models like ΛCDM and the quintessence model (Q-model) [66] at late times.

VIII. THERMODYNAMIC ANALYSIS

In this section, we discuss the validity of the generalized second law (GSL) of thermodynamics in the present model dominated by matter creation. It is to be noted that according to thermodynamics, the entropy of isolated systems can never diminish. We explore the calculations of total entropy S for the matter creation model. We assume that the apparent horizon is related to temperature and entropy analogous with the black hole event horizon [67]. So, according to GSL, the total entropy S must include the

entropy of all sources. During the evolution of the Universe, the rate of the entropy change of the fluid within the Universe and that of the horizon must always be greater than or equal to zero. As we are studying only recent and future times, the total entropy is equal to the sum of the contribution of entropy to matter S_m and the apparent horizon S_h, i.e., $S = S_m + S_h$, where $S_h = \frac{\kappa_B A}{4 l_{\text{Pl}}^2}$ is the entropy of the apparent horizon and S_m is the entropy of pressureless matter. A and l_{Pl} are the area of the horizon and Planck's length, respectively, and κ_B is the Boltzman constant. The area of the apparent horizon is given by $A = 4\pi r_h^2$, where $r_h = \frac{1}{\sqrt{(H^2 + ka^{-2})}}$. As we are restricting our analysis to a spatially flat model ($k = 0$), this assumption yields $r_h = H^{-1}$. Therefore, the horizon entropy reads as

$$S_h = \frac{\kappa_B \pi}{l_{\text{Pl}}^2 H^2}. \tag{60}$$

Using Eq. (22), the first derivative of Eq. (60) gives

$$\dot{S}_h = \frac{\kappa_B \pi H_0}{l_{\text{Pl}}^2} \frac{H_0}{H^2} (\epsilon + 3(1 - \beta - \gamma)) a^{-\frac{\epsilon + 3(1-\beta)}{2}}. \tag{61}$$

It is observed from the above equation that $\dot{S}_h \geq 0$ for $0 < \beta + \gamma \leq 1$. The matter entropy inside the dynamical apparent horizon is described by the Gibbs relation [68]:

$$T dS_m = d(\rho V) + p dV, \tag{62}$$

where $V = \frac{4\pi}{3} r_h^3$ is the spatial volume enclosed by the horizon and T is the temperature of the fluid, and we assume that the temperature T is equal to the temperature at the horizon T_h, where $T_h = 1/2\pi r_h$ [69].

Using Eq. (19), the above equation gives

$$\dot{S}_m = \frac{8\pi^2 H_0 \rho}{H^4} \left[\frac{(3\gamma - (\epsilon + 3(1 - \beta)))}{2} a^{-\frac{\epsilon + 3(1-\beta)}{2}} + \epsilon H \right]. \tag{63}$$

As H and ρ are positive, the positivity of $\dot{S}_m$ is ensured whenever $\epsilon + 3(1 - \beta) < 3\gamma$. Adding Eqs. (61) and (63), we get $\dot{S}_h + \dot{S}_m \geq 0$, provided $0 < (\beta + \gamma) < 1$ and $\epsilon + 3(1 - \beta) < 3\gamma$. This means that GSL is always valid with these constraints.

IX. CONCLUSION

In this paper, we have studied a matter-dominated model with "adiabatic" matter creation in Brans-Dicke theory with matter creation rate $\Gamma = 3\gamma H_0 + 3\beta H$ to explain the late-time accelerated expansion of the Universe. We have demonstrated how matter creation works well with the expanding Universe. In order to constrain the model parameters, statistical analyses using cosmic observations data from SNe, OHD, and BAO have been performed. Further, in order to reduce the number of the free variables,

we select to use the present value of the Hubble function, i.e., $H_0 = 67.8 \text{ km sec}^{-1} \text{ Mpc}^{-1}$. The results are given in Tables I and II. In Figs. 1–4, we have plotted the contour maps obtained from the datasets. According to the MCMC analysis, it is found that the best-fitting values of model parameters from SNe and SNe + BAO are little different than those obtained from SNe + OHD and SNe+ OHD + BAO. The later best-fit values are compatible with the ΛCDM model.

Using the best-fit values, we plot the evolutions of the scale factor, the deceleration parameter, and the effective equation of state parameter. From Fig. 5, it has been found that the model starts from a big bang followed by decelerated expansion at early times, with a transition to an accelerated epoch at later times, corresponding to the defined constraints. In some other constraints, the model predicts an eternally expanding universe, beginning with a big bang in the past followed by decelerated expansion and a smooth transition to an accelerated expansion. Table II gives the transition point a_{tr} from best-fitted values obtained from different datasets.

We have also discussed the evolution of the deceleration parameter q and the effective equation of state w_{eff}. From Fig. 6, it is observed that there is a transition from the decelerated phase to the accelerated phase. The present-day value of q_0 and transition redshift are found from each observational dataset. In general, $q \to -1$ as $a \to \infty$, which corresponds to a de Sitter model of the Universe. We have also plotted the trajectories for w_{eff} for best-fitted values of parameters in Fig. 7. In each case, the model does not cross the phantom divide line. Irrespective of the values of parameters, $w_{\text{eff}} \to -1$ as $z \to -1$.

The Hubble function of the model with error bar fits into the ΛCDM model for best-fitted values obtained from SNe + OHD and SNe + OHD + BAO (see Fig. 8). The age of the Universe obtained from SNe + OHD and SNe + OHD + BAO for best-fitting values is the same as that predicted by the ΛCDM model. However, it is comparatively higher than those obtained from SNe and SNe+ BAO, as shown in Fig. 9.

We have discussed the statefinder diagnostic for the model. In Fig. 10, we have plotted the trajectory of $\{r, s\}$ in the $s - r$ plane. The trajectory is different from that of the ΛCDM model. The model shows quintessence-like behavior. However, as $a \to \infty$, the statefinder parameter $\{r, s\} \to \{1, 0\}$ corresponds to the ΛCDM point.

We have analyzed the validity of GSL in the present model and found that the GSL of thermodynamics is valid with the apparent horizon as the boundary for $0 < (\beta + \gamma) < 1$ and $\epsilon + 3(1 - \beta) < 3\gamma$.

In summary, it is clear that the present work keeps itself in the domain of cosmology, and more specifically, in accelerating cosmology, which is a certain plight to understand the evolution of the Universe.

[1] A. G. Riess *et al.*, Astron. J. **116**, 1009 (1998); Astrophys. J. **607**, 665 (2004).

[2] S. Perlmutter *et al.*, Astrophys. J. **517**, 565 (1999).

[3] D. J. Eisenstein *et al.*, Astrophys. J. **633**, 560 (2005).

[4] D. N. Spergel *et al.*, Astrophys. J. Suppl. Ser. **170**, 377 (2007).

[5] S. Weinberg, Rev. Mod. Phys. **61**, 1 (1989).

[6] E. J. Copeland, M. Sami, and S. Tsujikawa, Int. J. Mod. Phys. D **15**, 1753 (2006).

[7] S. Capozziello, Classical Quantum Gravity **23**, 1205 (2006).

[8] Y. Zhang and Y. X. Gui, Classical Quantum Gravity **23**, 6141 (2006).

[9] Z. K. Guo, Y. S. Piao, X. M. Zhang, and Y. Z. Zhang, Phys. Lett. B **608**, 177 (2005).

[10] T. Chiba, T. Okabe, and M. Yamaguchi, Phys. Rev. D **62**, 023511 (2000).

[11] C. J. Feng, Phys. Lett. B **670**, 231 (2008).

[12] M. O. Calvao, J. A. S. Lima, and I. Waga, Phys. Lett. A **162**, 223 (1992).

[13] R. J. Scherrer, Phys. Rev. Lett. **93**, 011301 (2004).

[14] R. R. Caldwell, M. Kamionkowski, and N. N. Weinberg, Phys. Rev. Lett. **91**, 071301 (2003).

[15] A. Vikman, Phys. Rev. D **71**, 023515 (2005).

[16] L. P. Chimento and M. G. Richarte, Eur. Phys. J. C **73**, 2352 (2013).

[17] G. B. Zhao, Phys. Rev. D **72**, 123515 (2005).

[18] H. Wei and R. G. Cai, Phys. Lett. B **660**, 113 (2008).

[19] M. R. Setare, Phys. Lett. B **654**, 1 (2007).

[20] L. Amendola, Phys. Rev. D **62**, 043511 (2000).

[21] J. M. F. Maia and J. A. S. Lima, Phys. Rev. D **65**, 083513 (2002).

[22] S. Lee, G. C. Liu, and K. W. Ng, Phys. Rev. D **73**, 083516 (2006).

[23] I. Prigogine, J. Geheniau, E. Gunzig, and P. Nardone, Proc. Natl. Acad. Sci. U.S.A. **85**, 7428 (1988).

[24] I. Prigogine, J. Geheniau, E. Gunzig, and P. Nardone, Gen Relativ. Gravit. **21**, 767 (1989).

[25] J. A. S. Lima, A. S. M. Germano, and L. R. W. Abramo, Phys. Rev. D **53**, 4287 (1996).

[26] L. R. W. Abramo and J. A. S. Lima, Classical Quantum Gravity **13**, 2953 (1996).

[27] J. A. S. Lima, F. E. Silva, and R. C. Santos, Classical Quantum Gravity **25**, 205006 (2008).

[28] S. Basilakos and M. Plionis, Astron. Astrophys. **507**, 47 (2009).

[29] G. Steigman, R. C. Santos, and J. A. S. Lima, J. Cosmol. Astropart. Phys. 06 (2009) 033.

[30] J. A. S. Lima, J. F. Jesus, and F. A. Oliveira, J. Cosmol. Astropart. Phys. 11 (2010) 027.

[31] S. Basilakos and J. A. S. Lima, Phys. Rev. D **82**, 023504 (2010).

[32] C. P. Singh and A. Beesham, Astrophys. Space Sci. **336**, 469 (2011).

[33] C. P. Singh, Astrophys. Space Sci. **338**, 411 (2012).

[34] C. P. Singh, Mod. Phys. Lett. A **27**, 1250070 (2012).

[35] J. C. Fabris, J. A. F. Pacheco, and O. F. Piattella, J. Cosmol. Astropart. Phys. 06 (2014) 038.

[36] J. A. S. Lima, L. L. Gracf, D. Pavón, and S. Basilakos, J. Cosmol. Astropart. Phys. 10 (2014) 042.

[37] S. Chakraborty, S. Pan, and S. Saha, Phys. Lett. B **738**, 424 (2014).

[38] J. Haro and S. Pan, Classical Quantum Gravity **33**, 165007 (2016).

[39] S. Pan and S. Chakraborty, Adv. High Energy Phys. **15**, 654025 (2015).

[40] R. C. Nunes and D. Pavón, Phys. Rev. D **91**, 063526 (2015).

[41] T. Harko, F. S. N. Lobo, J. P. Mimoso, and D. Pavón, Eur. Phys. J. C **75**, 386 (2015).

[42] P. Kumar and C. P. Singh, Astrophys. Space Sci. **357**, 120 (2015).

[43] V. Singh and C. P. singh, Int. J. Theor. Phys. **55**, 1257 (2016).

[44] C. Brans and R. H. Dicke, Phys. Rev. **124**, 925 (1961).

[45] B. Bertotti, L. Iess, and P. Tortora, Nature (London) **425**, 374 (2003).

[46] Y. Gong, Phys. Rev. D **61**, 043505 (2000).

[47] H. Kim, Mon. Not. R. Astron. Soc. **364**, 813 (2005).

[48] S. Weinberg, *Gravitational and Cosmology: Principles and Applications of the General Theory of Relativity* (Wiley, New York, 1972), p. 622.

[49] G. Steigman, R. C. Santos, and J. A. S. Lima, J. Cosmol. Astrophys. Phys. 06 (**2009**) 033.

[50] N. Banerjee and D. Pavon, Phys. Lett. B **647**, 477 (2007).

[51] A. Sheykhi, Phys. Rev. D **81**, 023525 (2010).

[52] D. Foreman-Mackey, D. W. Hogg, D. Lang, and J. Goodman, Publ. Astron. Soc. Pac. **125**, 306 (2013).

[53] P. A. R. Ade et al., Astron. Astrophys. **594**, A13 (2016).

[54] M. Betoule et al., Astron. Astrophys. **568**, A22 (2014).

[55] R. Jimenez and A. Loeb, Astrophys. J. **573**, 37 (2002).

[56] S. L. Cao, H.-Y. Teng, H.-Y. Wan, H.-R. Yu, and T.-J. Zhang, Eur. Phys. J. C **78**, 313 (2018).

[57] N. Padmanabhan, X. Xu, D. J. Eisenstein, R. Scalzo, A. J. Cuesta, K. T. Mehta, and E. Kazin, Mon. Not. R. Astron. Soc. **427**, 2132 (2012).

[58] F. Beutler, C. Blake, M. Colless, D. Heath Jones, L. Staveley-Smith, L. Campbell, Q. Parker, W. Saunders, and F. Watson, Mon. Not. R. Astron. Soc. **416**, 3017 (2011).

[59] L. Anderson et al., Mon. Not. R. Astron. Soc. **441**, 24 (2014).

[60] C. Blake et al., Mon. Not. R. Astron. Soc. **425**, 405 (2012).

[61] R. Giostri, M. Vargas dos Santos, I Waga, R. R. R Reis, M. O. Calvão, and B. L. Lago, J. Cosmol. Astropart. Phys. 03 (2012) 027.

[62] G. Hinshaw et al., Astrophys. J. Suppl. Ser. **208**, 19 (2013).

[63] P. Praseetha and T. K. Mathew, Int. J. Mod. Phys. D **23**, 1450024 (2014).

[64] E. Komatsu et al. (WMAP Collaboration), Astrophys. J. Suppl. Ser. **192**, 18 (2011).

[65] C. J. Feng and X. Z. Li, Phys. Lett. B **680**, 355 (2009).

[66] V. Sahni, T. D. Saini, A. A. Starobinsky, and U. Alam, JETP Lett. **77**, 201 (2003).

[67] R.-G. Cai, L.-M. Cao, and Y.-P. Hu, Classical Quantum Gravity **26**, 155018 (2009).

[68] G. Izquierdo and D. Pavón, Phys. Lett. B **639**, 1 (2006).

[69] M. Akbar and R. G. Cai, Phys. Rev. D **75**, 084003 (2007).